IEEE Photonics Journal
An IEEE Photonics Society Publication

Gain Improvement of Er-Ti:$LiNbO_3$ Waveguide Amplifier by an As_2S_3 Overlay Waveguide

Volume 3, Number 4, August 2011

X. Song
W. Tan
W. T. Snider
X. Xia, Member, IEEE
C. K. Madsen, Member, IEEE

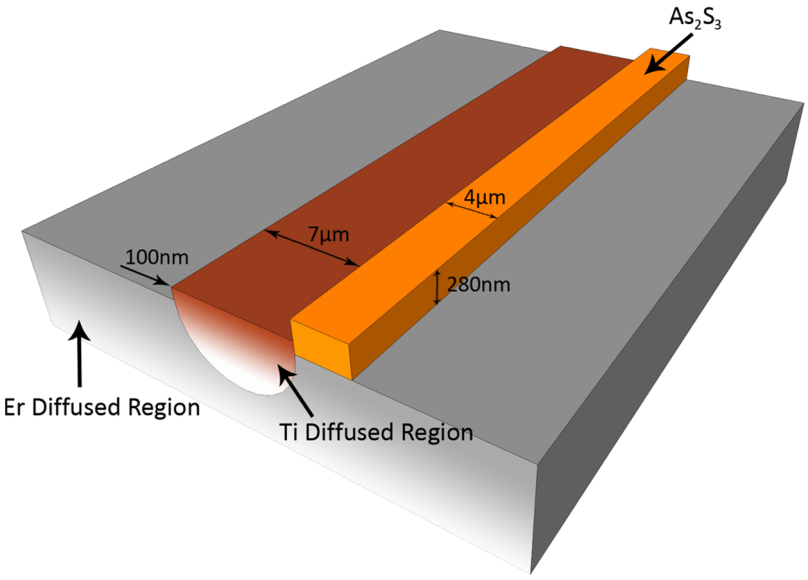

DOI: 10.1109/JPHOT.2011.2160529
1943-0655/$26.00 ©2011 IEEE

Gain Improvement of Er-Ti:$LiNbO_3$ Waveguide Amplifier by an As_2S_3 Overlay Waveguide

X. Song, W. Tan, W. T. Snider, X. Xia, *Member, IEEE,*
C. K. Madsen, *Senior Member, IEEE,*

Department of Electrical and Computer Engineering, Texas A&M University, College Station, TX 77843 USA

DOI: 10.1109/JPHOT.2011.2160529
1943-0655/$26.00 ©2011 IEEE

Manuscript received May 10, 2011; revised June 18, 2011; accepted June 18, 2011. Date of publication June 27, 2011; date of current version July 15, 2011. This work was supported by the National Science Foundation and the Defense Advanced Research Projects Agency. Corresponding author: X. Song (e-mail: songxm99@neo.tamu.edu).

Abstract: A new configuration consisting of an arsenic trisulfide (As_2S_3) channel waveguide on top of an erbium (Er)-doped titanium-diffused *x*-cut lithium niobate (Er:Ti:$LiNbO_3$) waveguide has been investigated by simultaneous analytical expressions, numerical simulations, and experimentation. Both simulation and experimental results have shown that this structure can enhance the optical gain, as predicted by the analytical expressions. An As_2S_3 channel waveguide has been fabricated on top of a conventional Er:Ti:$LiNbO_3$ waveguide, where the higher refractive index As_2S_3 waveguide is used to pull the optical mode toward the substrate surface where the higher Er concentration yields an improved propagation gain. The relationship between the gain and As_2S_3 layer thickness has been evaluated, and the optimal As_2S_3 thickness was found by simulation and experimentation. Side integration was applied to reduce the extrapropagation loss caused by the titanium diffusion bump. The propagation gain has been improved from 1.1 to 2 dB/cm.

Index Terms: Arsenic trisulfide, erbium (Er)-doped waveguide amplifiers, titanium-diffused lithium niobate.

1. Introduction

Erbium (Er)-doped Ti:$LiNbO_3$ waveguides have been extensively investigated [1]. The overlap between the optical fields and Er ions has been related to the optical gain [2], which has been achieved to overcome the propagation loss and even high enough to make lasers [3]–[5]. It is well known that the propagation gain is proportional to the overlap between the optical mode and Er profile.

For the surface in-diffused Er profile, achieving a high overlap requires pulling the optical mode closer to the surface, where the Er concentration is higher. To achieve the mode pulling, a blanket-clad TiO_2 configuration has been reported with estimates on the gain improvement [6]. Arsenic trisulfide (As_2S_3) is a better choice for mode pulling, owing to its high refractive index. Other benefits include a high nonlinear coefficient, low propagation loss, and low processing temperature. In this paper, we focus on the gain improvement by using a patterned As_2S_3 waveguide on top of a straight Er:Ti:$LiNbO_3$ to elevate the mode. As illustrated by Figs. 1 and 12, utilizing a straight channel As_2S_3 waveguide instead of a blanket film not only improves the gain but reduces the propagation loss by side coupling as well. We have found that surface roughness from the Ti-diffused bump will introduce excess losses if the As_2S_3 waveguide sits on top of the diffused waveguide. Hence, the As_2S_3 layer

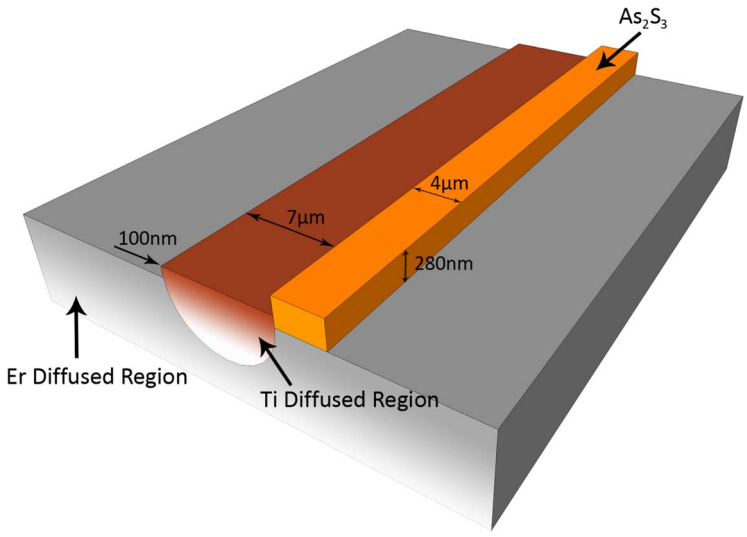

Fig. 1. Schematic picture of our structure.

is patterned next to the titanium bump to utilize side coupling and avoid the losses associated with the nonplanar bump surface. Furthermore, the patterned As_2S_3 waveguide enables vertically integrated structures, which combines the As_2S_3 waveguide above the substrate surface and the Er:Ti:$LiNbO_3$ waveguide below the surface, such as Mach–Zehnder interferometers (MZIs) and rings [7], [8].

Recent research has shown that As_2S_3 rings can be coupled with Ti:$LiNbO_3$ waveguides to implement filtering functions by top coupling [7] and side coupling [8]. Our structure can be integrated with the ring to compensate for propagation losses, making the ring lossless which has further potential applications [9]. Since the rings are designed to operate with TM polarization [7], [8], [10], we mainly focus on investigating TM polarization through simulations and experiments for our As_2S_3-assisted Er:Ti:$LiNbO_3$ structure while the TE polarization simulation is also performed.

We also investigated the range of As_2S_3 thicknesses that enhance the optical gain, and found the optimum As_2S_3 waveguide parameters through simulations and confirmed in experimentation.

2. Analytical Expression

The gain of the amplifier is a function of the overlap between the Er profile and optical mode. In the two-level model, the steady state propagation equation describing the signal power evolution in the optical amplifier is given by [11], [12]

$$\partial P_s(z)/\partial z = (\gamma_{21} - \gamma_{12})P_s(z) - \alpha P_s(z) \tag{1}$$

$$\gamma_{21} = N_2(z) \iint_A \Psi_s(x,y)\sigma_s^e \rho Er(x,y)\, dx\, dy \tag{2}$$

$$\gamma_{12} = N_1(z) \iint_A \Psi_s(x,y)\sigma_s^a \rho Er(x,y)\, dx\, dy \tag{3}$$

$$\iint_A \Psi_s(x,y)\, dx\, dy = 1 \tag{4}$$

where P_s is the signal power, and Ψ_s is the normalized mode distribution. γ_{21} and γ_{12} are expressed by (2) and (3). ρ is the density of Er atoms at the $LiNbO_3$ surface, and $Er(x,y)$ is the normalized diffused Er profile, where the maximum of $Er(x,y) = 1$. σ_s^e and σ_s^a are the cross sections for

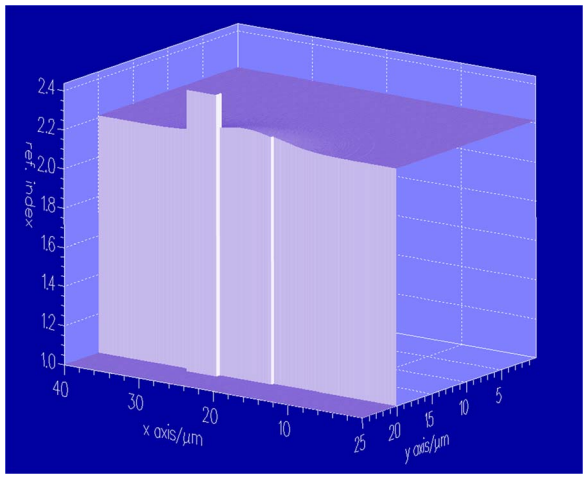

Fig. 2. Refractive index profile for TM mode. Z-axis is refractive index (1.0–2.4); x-axis is waveguide width (0–40 μm); y-axis is waveguide depth (0–25 μm).

stimulated emission and absorption at signal wavelength. $N_2(z)$ and $N_1(z)$ are the fraction of atoms per unit length in the excited state and ground state ($N_2(z) + N_1(z) = 1$ [12]), which are determined by the pump efficiency. Here, the amplified spontaneous emission (ASE) noise is ignored since the gain is small. We assumed that the pump power is high enough ($>$ 20 dBm) to maximize the population inversion of the Er atoms so that the gain is uniform along the waveguide. Substituting (2)–(4) into (1) becomes

$$\partial P_s(z)/\partial z/P_s(z) = \rho\Gamma\left[\left(\sigma_s^e + \sigma_s^a\right)N_2(z) - \sigma_s^a\right] - \alpha_s \tag{5}$$

$$\Gamma = \iint_A \Psi_s(x,y)Er(x,y)\,dx\,dy \tag{6}$$

where Γ expressed by (6) is the overlap between the normalized signal mode Ψ_s and the Er profile $Er(x,y)$, and α_s is the propagation loss.

The optical gain (decibels per unit length) can be expressed by inserting the conversion factor $10\log(e)$ into (5) [12]. The propagation gain (gain per unit length) is defined as the gain relative to the non-Er-doped waveguide, which has loss α_s, as follows:

$$Gain(dB/l) = 10\log(e)\rho\Gamma\left[\left(\sigma_s^e + \sigma_s^a\right)N_2(z) - \sigma_s^a\right] \tag{7}$$

Therefore, the propagation gain is proportional to the overlap between the signal mode and Er profile.

3. Simulation

We used FIMMWAVE, by Photon Design Ltd., to solve the optical modes by film mode matching (FMM) method at 1531 nm for the signal and 1480 nm for the pump. Fig. 1 shows the structure of the vertical integration between Er:Ti:LiNbO$_3$ and As_2S_3 waveguides. The device is made on an x-cut y-propagation lithium niobate substrate with planer-diffused Er. The titanium-diffused waveguide is in the center, while the As_2S_3 waveguide is placed next to it above the surface.

Fig. 2 illustrates the refractive index profile of the waveguide. The index value is shown in z-axis and the waveguide cross section is shown in x–y plane. Corresponding to the structure in Fig. 1, the As_2S_3 waveguide is represented by the protruding pole $(n = 2.4)$ with the bump next to it, on which the swelled part is the titanium-diffused region in lithium niobate substrate (the bulk part, $n_{TM} = 2.21 + \Delta n_{Ti-diffused-TM}$, $n_{TE} = 2.13 + \Delta n_{Ti-diffused-TE}$). The air cladding $(n = 1)$ is at the bottom.

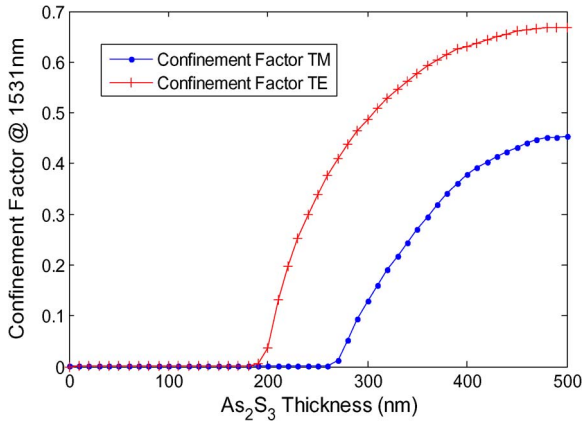

Fig. 3. Confinement factor in As_2S_3 at signal wavelength (1531 nm) for both TM and TE modes.

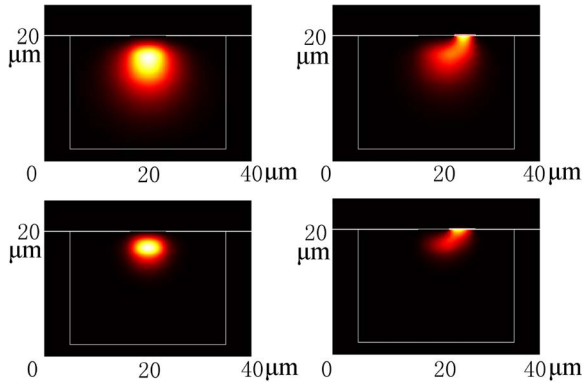

Fig. 4. (1) (Top left) TM mode without As_2S_3. (2) (Top right) TM mode with 0.28-μm-thick As_2S_3. (3) (Bottom left) TE mode without As_2S_3. (4) (Bottom right) TE mode with 0.28-μm-thick As_2S_3.

As we swept the dimensions of the As_2S_3 waveguide, we found that the thickness of the As_2S_3 thin film is the most sensitive parameter. The As_2S_3 width must be larger than 2 μm to pull up the mode, but further increasing the width to infinity only changes the overlap by 17%. However, changing the thickness from 0 to 0.5 μm changes the overlap by 230%. Therefore, we set the As_2S_3 width to 4 μm and subsequently swept the thickness.

The resulting confinement factor which is the percentage of optical intensity in As_2S_3 is shown in Fig. 3. It increases with the As_2S_3 waveguide thickness.

The Er profile was measured by Secondary Ion Mass Spectrometry (SIMS) in Fig. 11. The effective depth is $d_{eff} = 4.9$ μm after fitting for the complementary error function. Using the optical modes and Er profile, the overlap integral Γ between the modes and Er profile expressed by (6) can be simulated. Fig. 4 shows the simulated mode profiles and the mode pulling effect. Having considered the overlap between the mode and Er (see Fig. 5), and pump effects (see Figs. 6–10), the optimum thicknesses for transverse magnetic (TM) and transverse electric (TE) are found to be 280 nm and 200 nm, respectively.

Fig. 5 shows the overlap of the signal modes and Er profile. We normalized all the overlap data relative to the overlap when the As_2S_3 thickness equals to zero. For TM mode, the overlap starts from 1 and increases slowly at 0–0.2 μm but changes dramatically at 0.25–0.3 μm. After 0.3 μm, it falls. After 0.5 μm, it falls below 1 since 45% power of mode has spread into the As_2S_3 area and cannot be pumped since there is no Er there. The mode is overpulled. The overlap for the TE mode shows a similar curve, with the peak at 0.21 μm.

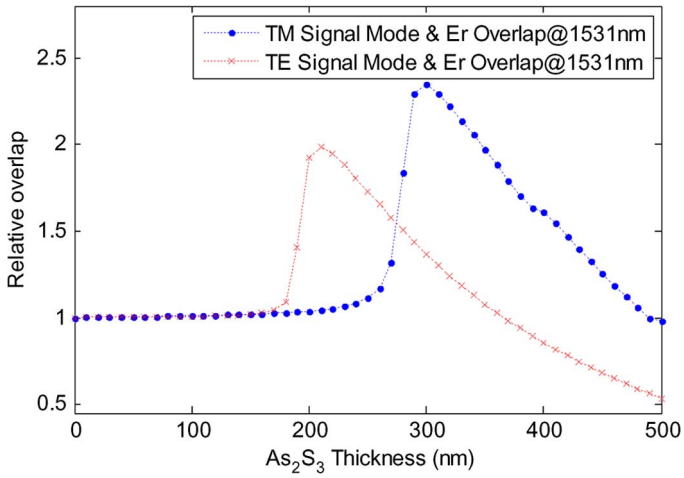

Fig. 5. Overlap Data. Signal modes and Er overlap.

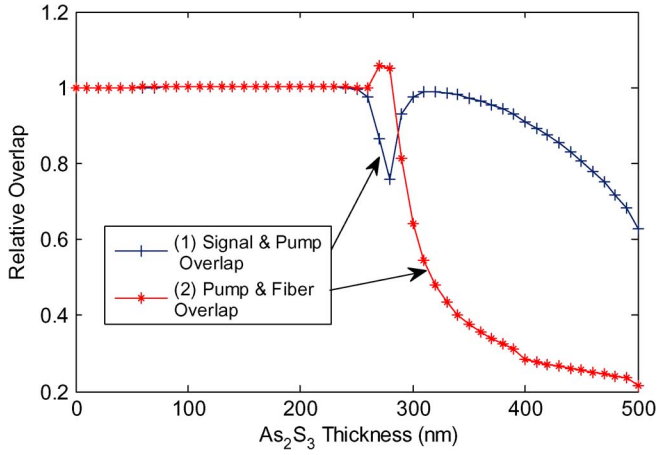

Fig. 6. Pump effects for TM mode. (1) Pump and signal mode overlap. (2) Pump and fiber modes overlap.

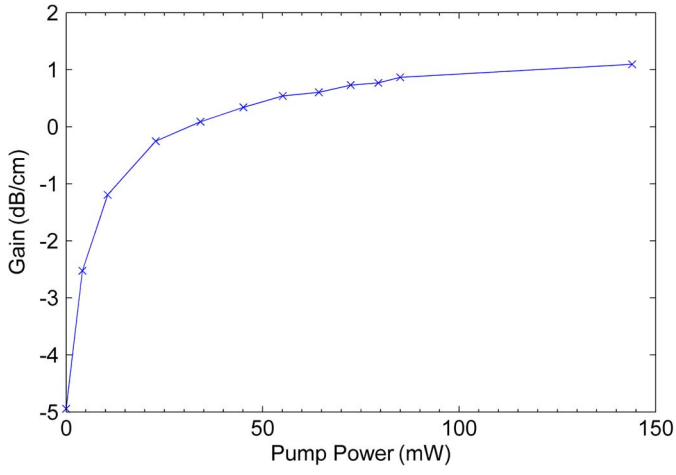

Fig. 7. Propagation Gain versus pump power for Er:Ti:LiNbO3 waveguide without As2S3 for TM mode. Sample fabrication parameters are discussed in Section 4, and the measurement setup is discussed in Section 5.

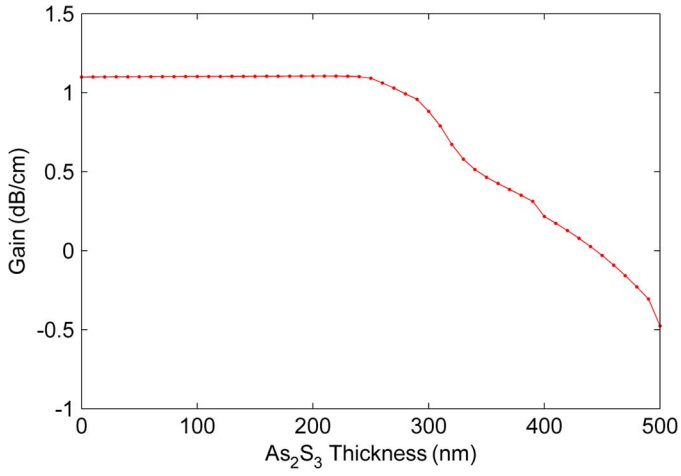

Fig. 8. Effective gain influenced by Pump effects for TM mode.

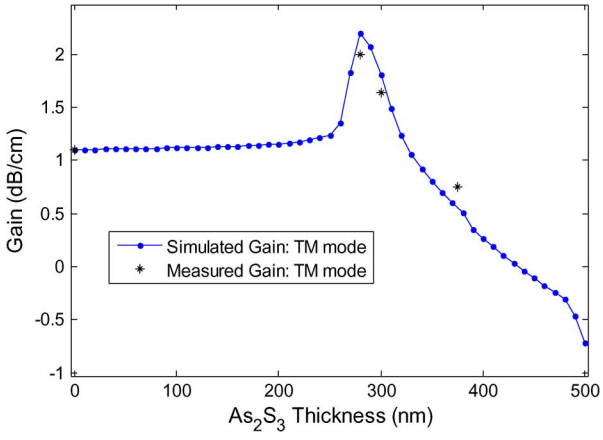

Fig. 9. Propagation gain versus As_2S_3 thickness. Comparing measured and simulated results for TM mode: peak at 280 nm.

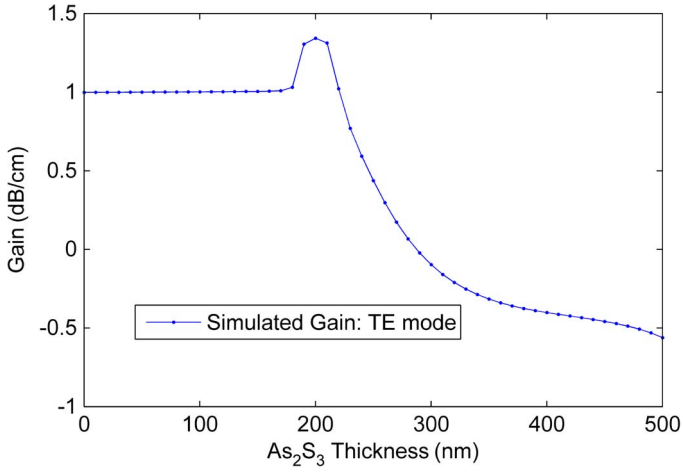

Fig. 10. Propagation gain versus As_2S_3 thickness. Simulated results for TE mode: peak at 200 nm.

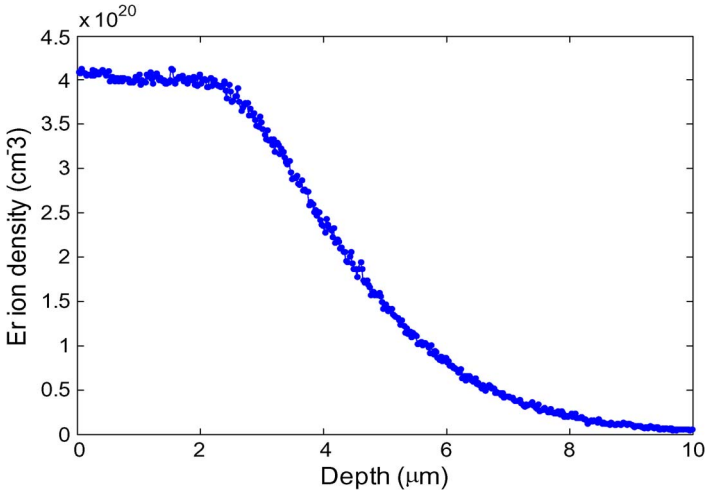

Fig. 11. Er concentration profile measured by Secondary Ion Mass Spectrometry (SIMS).

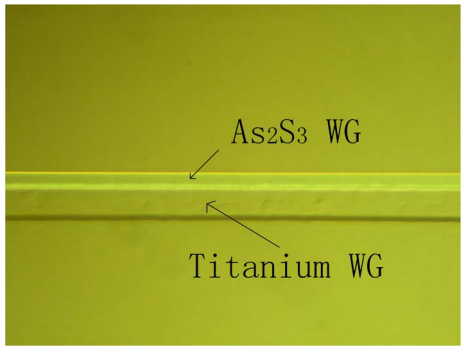

Fig. 12. Top-view photomicrograph of Ti:$LiNbO_3$ and As_2S_3 waveguides (WG).

The As_2S_3 waveguide not only enhances the modes and Er overlap but influences the pump to signal mode mismatch O_{SP} and pump to fiber modes coupling O_{PF} as well. They are defined in (8) and (9) and plotted as curves in Fig. 6

$$O_{S\&P} = \iint_A \Psi_s(x,y)\Psi_P(x,y)\,dx\,dy \tag{8}$$

$$O_{P\&F} = \iint_A \Psi_p(x,y)\Psi_f(x,y)\,dx\,dy \tag{9}$$

where Ψ_s, Ψ_p, and Ψ_f are the signal, pump, and fiber modes. The fiber mode has a mode field diameter (MFD) of 9.9 μm at 1480 nm, measured by the beam profiler.

These pump-related overlaps change the amount of pump power interacting with Er ions and the signal mode. They impact pump efficiency and, thus, are similar to changing the input pump power. We multiply these two overlap values and take the product as the pump efficiency ratio. Experimentally, we measured the gain versus pump power, shown in Fig. 7, for the waveguide without As_2S_3. Therefore, the effective gain in Fig. 8 is computed from the gain versus pump power curve in Fig. 7, while the effective pump power is calculated by multiplying the pump efficiency ratio and pump power (144 mW).

Based on (7), this gain should be proportional to the signal mode and Er overlap. As shown in Fig. 9, the final simulated propagation gain versus As_2S_3 thickness is obtained as the product of the

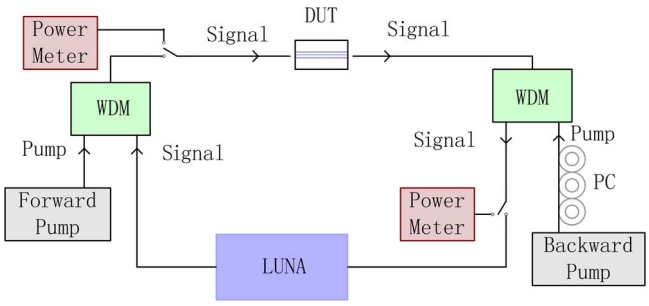

Fig. 13. Schematic of the propagation gain measurement.

curves in Figs. 5 and 8. From Fig. 6, the optimum thickness for gain is found to be 0.28 μm, which is a -0.2 μm shift from Fig. 5 due to pump effects. Our experimental data for several As_2S_3 thicknesses is also plotted, and it matches well with the simulated curve. The same process can be performed for TE polarization and the final simulated gain is plotted in Fig. 10. The optimum thickness is 0.20 μm, which is a 0.1-μm shift from Fig. 5 due to pump effects.

4. Fabrication

A 13-nm-thick Er layer was sputtered onto a 3-cm-long *x*-cut, *y*-propagating $LiNbO_3$ substrate and diffused at 1100 °C for 120 hr. The resulting Er profile measured by SIMS is shown in Fig. 11. Then, a 95-nm titanium film was sputtered, patterned, and diffused for 9.5 hr in wet breathing air ambient. The end facets of the waveguide chip were then polished to optical quality, and the Er:Ti:$LiNbO_3$ waveguide tested by butt-coupling single-mode fibers. The mode profiles were shown in Fig. 4. The mode field diameter (MFD) is defined as the full width at $1/e^2$ for mode intensity profile. They are measured for TM mode (vertical: 10.7 μm, horizontal: 13.9 μm) and TE mode (vertical: 5.6 μm, horizontal: 8.6 μm). After that, a thin film of As_2S_3 (refractive index: 2.4) was deposited using radio frequency magnetron sputtering at varying thicknesses (0 nm, 280 nm, 300 nm, and 375 nm) with a constant 4-μm width. The top view in Fig. 12 shows that the As_2S_3 waveguide is placed next to the bump of the titanium-diffused waveguide to keep the As_2S_3 waveguide away from the rough surface of the bump.

5. Experiment Result

A schematic of the measurement setup for the optical gain is detailed in Fig. 13. We use the optical vector analyzer (OVA), by Luna Technologies, which has a built-in wavelength swept source (left port) and detector (right port). It can scan the loss (or gain) of the device under test (DUT) over a wavelength range 1520–1608 nm for both TM and TE polarizations.

The forward pump laser power is 59 mW, the backward pump laser power is 85 mW before being launched into the waveguide, and the pump wavelength is 1480 nm. The backward pump was TM polarized to increase the overlap with the signal mode. Signal and pump are combined by two WDM couplers. Two power meters are used to separately optimize fiber-to-device alignment and pump polarization.

There is only a small difference for measured insertion losses with the pump on and off for wavelengths longer than 1590 nm. Thus, the pump has little effect for this wavelength range, and we use the average value for the pump on and off conditions as the absolute reference for the propagation gain calculation. Note, our Ti:$LiNbO_3$ waveguide loss has negligible wavelength dependence ($\sim$0.1 dB variation over 1520–1605 nm). The propagation gain is extracted directly from the spectral data of the waveguide itself, avoiding uncertainties in estimating the fiber-to-waveguide coupling loss in the gain calculation.

First, we measured the Er:Ti:$LiNbO_3$ waveguide without an As_2S_3 layer. Then, we fabricated an As_2S_3 waveguide on top. The best gain was found with an As_2S_3 thickness of 280 nm (see Fig. 9). The propagation gain was enhanced by 0.9 dB/cm from 1.1 to 2 dB/cm (see Fig. 14). The peak

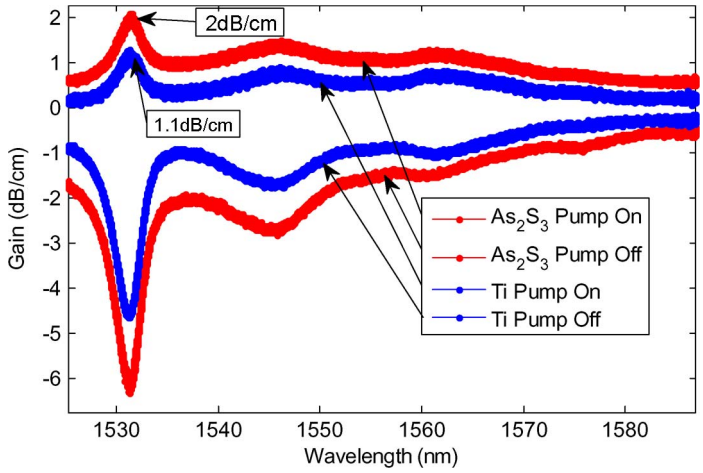

Fig. 14. Propagation gain spectrum with and without As_2S_3 on $LiNbO_3$ for TM mode (As_2S_3 thickness = 280 nm).

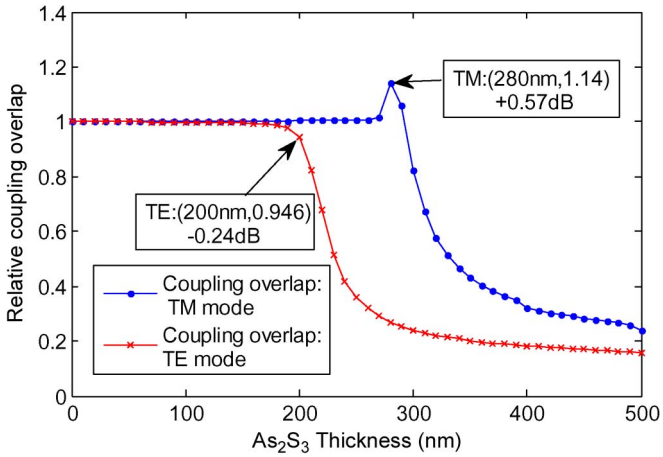

Fig. 15. Coupling overlap (coupling loss) for TM and TE modes.

amplification wavelength is at 1531 nm. Compared with the case without the As_2S_3 waveguide, the propagation gain in the Er:Ti:$LiNbO_3$ waveguide with the As_2S_3 waveguide has been improved substantially for the same launched pump power conditions, as predicted by simulation. Taking into account propagation loss (0.4 dB/cm for TM mode) and coupling losses, the net gain for this 3-cm-long sample has been improved from 1.1 dB to 3.5 dB.

Our approach provides the opportunity for enhanced device functionality. As one example, the As_2S_3 channel waveguides can become part of a vertically integrated ring resonator, enabling the signal to be amplified and potentially compensate the ring's roundtrip loss. Thus, ideal all-pass filters may be realized in the future, as well as hi-Q, gain-tuned rings.

6. Discussion

Coupling losses between the mode and the fiber must be considered since the mode shape is changed. The coupling losses include Fresnel reflections, which are constant, and the mode shape mismatch, which is the overlap between the waveguide mode and fiber mode. The coupling losses of the Ti:Er:$LiNbO_3$ waveguide have been measured at 1531 nm for TM mode (0.5 dB) and TE mode (0.9 dB).

The waveguide modes for varying As_2S_3 thicknesses have been simulated at 1531 nm for both TM and TE polarizations. The fiber mode with Gaussian distribution has a mode field diameter

(MFD) of 10.2 μm at 1531 nm, measured by the beam profiler. The relative horizontal and vertical shifts between waveguide and fiber modes were scanned to achieve the best alignment. Fig. 15 shows the calculated coupling overlap data, which is normalized by the overlap without an As_2S_3 waveguide. The coupling overlap for an As_2S_3 thickness of 280 nm with TM polarization is 1.14 ($+$0.57 dB), normalized to the overlap with no As_2S_3, which is even better than the overlap without As_2S_3. This is because the TM mode for the 7-μm-wide Ti:$LiNbO_3$ waveguide is larger than fiber mode, but the As_2S_3 waveguide reduces the mode size and better matches the fiber mode, reducing coupling loses.

For TE polarization at 200 nm, the normalized coupling overlap is 0.946 ($-$0.24 dB). It can be overcome by introducing a tapered As_2S_3 waveguide [10]. The waveguide width can increase/decrease gradually from 0.5 μm to 4 μm in 3 mm length at the input/output ports of the waveguide. Therefore, the mode profile at the waveguide ends is the same as the normal Ti:$LiNbO_3$ waveguide mode, while in the center, it is the pulled-up by the As_2S_3 waveguide.

7. Conclusion

To conclude, we analyzed the gain improvement for various overlay geometries by relating the optical mode and Er overlap to the optical propagation gain. The optimal overlay thickness was found and confirmed by experiment. The propagation gain improved from 1.1 to 2 dB/cm at 1531 nm for the TM mode. This approach is compatible with vertical integration of high-index waveguides, with application to ring resonator-based filters where the roundtrip losses may be compensated with gain.

Acknowledgment

The authors wish to thank the anonymous reviewers for their valuable suggestions.

References

[1] R. Brinkmann, I. Baumann, M. Dinand, W. Sohler, and H. Suche, "Erbium-doped single and double pass Ti:$LiNbO_3$ waveguide amplifiers," *IEEE J. Quantum Electron.*, vol. 30, no. 10, pp. 2356–2360, Oct. 1994.
[2] M. Dinand and W. Sohler, "Theoretical modeling of optical amplification in Er-doped Ti:$LiNbO_3$ waveguides," *IEEE J. Quantum Electron.*, vol. 30, no. 5, pp. 1267–1276, May 1994.
[3] P. Becker, R. Brinkmann, M. Dinand, W. Sohler, and H. Suche, "Er diffused Ti:$LiNbO_3$ waveguide laser of 1563 and 1576 nm emission wavelengths," *Appl. Phys. Lett.*, vol. 61, no. 11, pp. 1257–1259, Sep. 1992.
[4] I. Baumann, R. Brinkmann, M. Dinand, W. Sohler, and S. Westenhöfer, "Ti:Er:$LiNbO_3$ waveguide laser of optimized efficiency," *IEEE J. Quantum Electron.*, vol. 32, no. 9, pp. 1695–1706, Sep. 1996.
[5] W. Sohler, B. Das, D. Dey, S. Reza, H. Suche, and R. Ricken, "Erbium-doped lithium niobate waveguide lasers," *IEICE Trans. Electron.*, vol. E88-C, no. 5, pp. 990–997, May 2005.
[6] K. Kishioka, T. Kishimoto, and K. Kume, "Improvement of the optical gain in the Er-doped lithium niobate waveguide optical amplifiers," *IEICE Trans. Electron.*, vol. E88-C, no. 5, pp. 1041–1052, May 2005.
[7] M. E. Solmaz, D. B. Adams, W. C. Tan, W. T. Snider, and C. K. Madsen, "Vertically integrated As_2S_3 ring resonator on$LiNbO_3$," *Opt. Lett.*, vol. 34, no. 11, pp. 1735–1737, Jun. 2009.
[8] Y. Zhou, X. Xia, W. T. Snider, J. H. Kim, Q. Chen, W. C. Tan, and C. K. Madsen, "Two-stage taper enhanced ultra-high Q-As_2S_3 ring resonator on $LiNbO_3$," *IEEE Photon. Technol. Lett.,* Jun. 2011.
[9] C. K. Madsen and G. Lenz, "Optical all-pass filters for phase response design with applications for dispersion compensation," *IEEE Photon. Technol. Lett.*, vol. 10, no. 7, pp. 994–996, Jul. 1998.
[10] X. Xia, Y. Zhou, and C. K. Madsen, "Analysis of As_2S_3-Ti:$LiNbO_3$ taper couplers using supermode theory," *J. Lightw. Technol.*, submitted for publication.
[11] A. A. M. Saleh, R. M. Jopson, J. D. Evankow, and J. Aspell, "Modeling of gain in erbium-doped fiber amplifiers," *IEEE Photon. Technol. Lett.*, vol. 2, no. 10, pp. 714–717, Oct. 1990.
[12] Y. Sun, J. L. Zyskind, and A. K. Srivastava, "Average inversion level, modeling, and physics of erbium-doped fiber amplifiers," *IEEE J. Sel. Topics Quantum Electron.*, vol. 3, no. 4, pp. 991–1007, Aug. 1997.